Entrained flow reactor (EFR)

Gavin Wiggins

June 9, 2020

Contents

1   Introduction

This report provides an overview of the Entrained Flow Reactor (EFR) at NREL and associated computational modeling tasks. The reactor operates at fast pyrolysis conditions to thermochemically convert biomass into gaseous products. The EFR is part of the Thermochemical Process Development Unit (TCPDU) at NREL which was originally designed for biomass gasification where the EFR was used as a thermal cracker. An overview of the TCPDU system is shown in Figure 1.
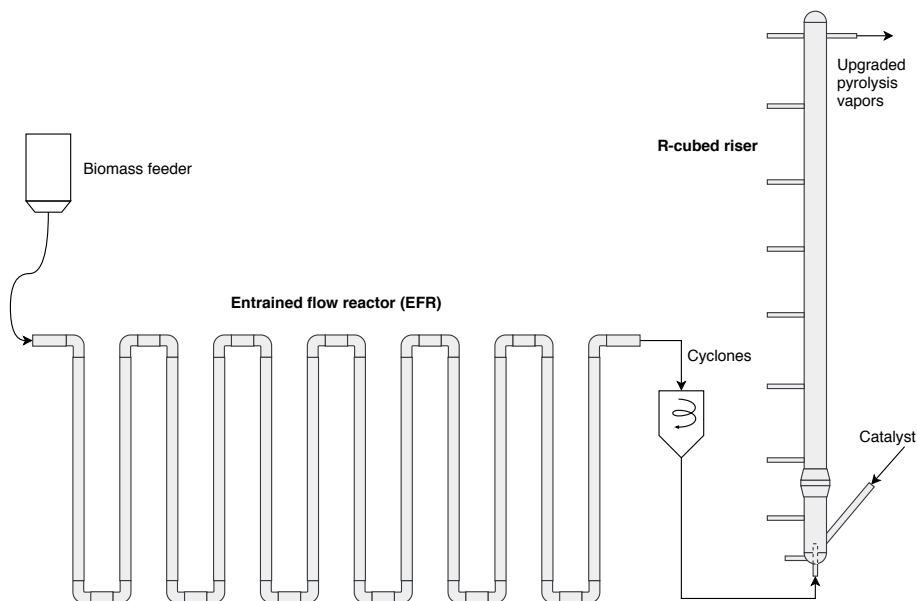

Figure 1: Overview of the main components of the NREL TCPDU system. Fast pyrolysis of biomass occurs in the entrained flow reactor. Catalytic vapor phase upgrading occurs in the R-cubed riser reactor.

2   Experimental setup

This section provides geometric dimensions and typical operating conditions for the entrained flow reactor. Characteristics for the Blend3 and forest residue feedstocks are also discussed.

2.1   Entrained flow reactor

Fast pyrolysis in the TCPDU system occurs in the entrained flow reactor (EFR) which is comprised of a series of horizontal and vertical pipes connected with 90 degree elbows (see Figure 2). The EFR is essentially a pneumatic conveyor

where biomass particles flow through a long pipe with several bends. Dimensions and material information about the EFR are provided in Figure 3 below. Operating conditions such as temperatures, pressures, and flow rates for the EFR are shown in Figure 4. Nitrogen gas at 500°C is generally used as the conveying medium for the solids.
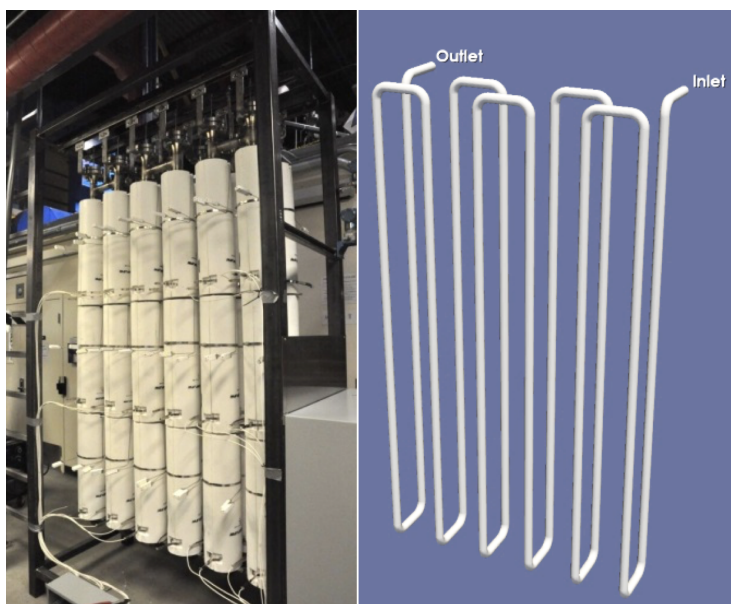

Figure 2: Left - picture of the EFR assembly with heat jackets, insulation, and thermocouples. Right - CAD representation of the EFR pipe assembly used for MFiX simulations.
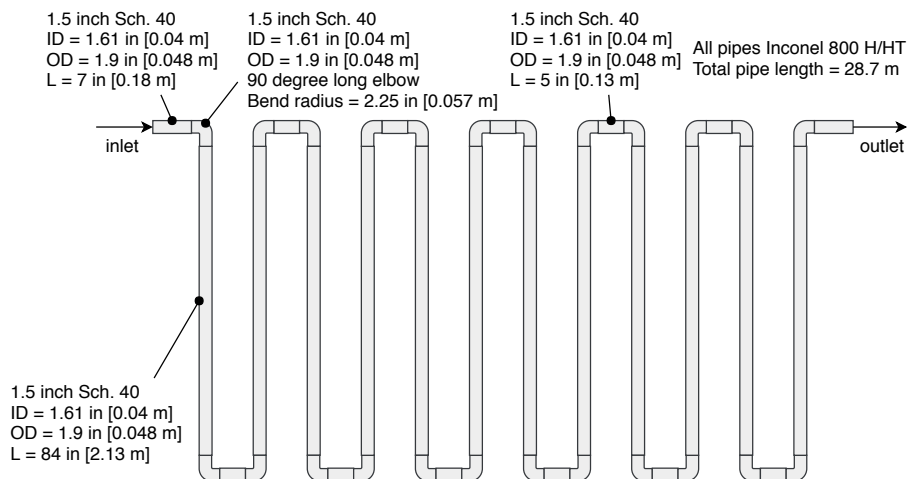
1.5 inch Sch. 40
ID = 1.61 in [0.04 m]
OD = 1.9 in [0.048 m]
L = 7 in [0.18 m]

1.5 inch Sch. 40
ID = 1.61 in [0.04 m]
OD = 1.9 in [0.048 m]
90 degree long elbow
Bend radius = 2.25 in [0.057 m]

1.5 inch Sch. 40
ID = 1.61 in [0.04 m]
OD = 1.9 in [0.048 m]
L = 5 in [0.13 m]

All pipes Inconel 800 H/HT
Total pipe length = 28.7 m

inlet

outlet

1.5 inch Sch. 40
ID = 1.61 in [0.04 m]
OD = 1.9 in [0.048 m]
L = 84 in [2.13 m]

Figure 3: Geometry of the entrained flow reactor at NREL.

nitrogen gas = 15 kg/hr, 500°C
biomass = 15 kg/hr
particle size = 2 mm sieve
pressure = 60.1 kPa

ΔP = 0.8 kPa
all pressures gauge

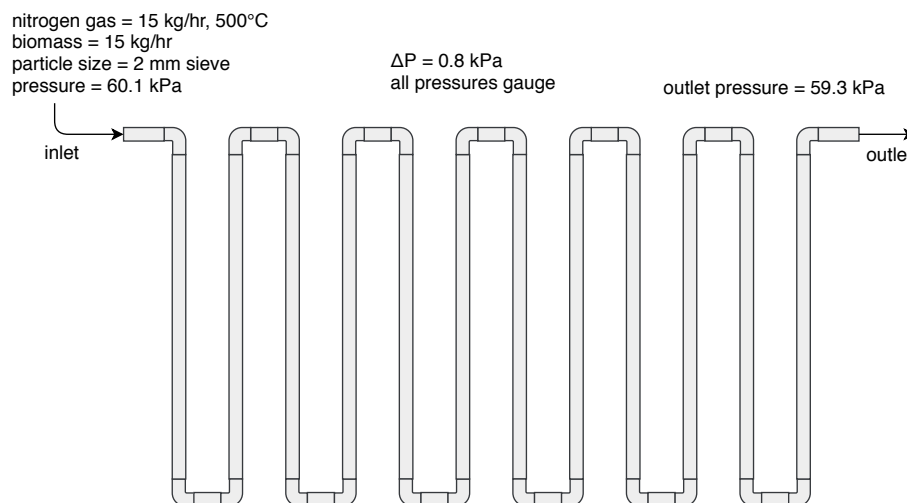outlet pressure = 59.3 kPa

inlet

outlet

Figure 4: Typical operating conditions for the entrained flow reactor.

2.2 Blend3 feedstock

General information about the Blend3 feedstock used in the entrained flow reactor is provided in Table 1. There is currently no information regarding identification of the feedstock or who performed the feedstock measurements and data preparation. Proximate and ultimate analysis data for the feedstock are presented in Tables 2 and 3. Only one set of analysis data is available therefore the uncertainty in the values is unknown.

4

Table 1: General information for the Blend3 feedstock.

Item	Description
Name	Blend3
ID	?
Contact	?

Table 2: Blend3 proximate analysis mass percent, as-received basis. Source [3].

Proximate	% ar	% ar	% ar
FC	16.92	?	?
VM	76.40	?	?
ash	0.64	?	?
moisture	6.04	?	?

Table 3: Blend3 ultimate analysis mass percent, as-received basis. Source [3].

Element	% ar	% ar	% ar
C	49.52	?	?
H	5.28	?	?
O	38.35	?	?
N	0.15	?	?
S	0.02	?	?
ash	0.64	?	?
moisture	6.04	?	?

The chemical analysis of the Blend3 feedstock is presented in Table 4. Again, only one set of data is available so the uncertainty in the measurements is unknown. The chemical analysis measurements are used to determine the biomass composition which is needed for the kinetics model.

Table 4: Blend3 chemical analysis mass percent, dry basis. Source [8].

Chemical component	% dry	% dry	% dry
glucan	38.95	?	?
acetyl	1.59	?	?
arabinan	1.40	?	?
galactan	3.16	?	?
mannan	10.52	?	?
xylan	7.89	?	?
lignin	29.48	?	?
free fructose	0.07	?	?
free glucose	0.04	?	?
sucrose	0.04	?	?
water extractives	2.75	?	?
ethanol extractives	3.49	?	?
non-structural inorganics	0.22	?	?
structural inorganics	0.41	?	?

Table 5: Blend3 ash analysis as weight percent of ash. Source [3].

Metal oxide	wt. %	wt. %	wt. %
SiO_2	28.1	?	?
Al_2O_3	7.06	?	?
TiO_2	0.34	?	?
CaO	21.8	?	?
Na_2O	0.71	?	?
K_2O	13.8	?	?
P_2O_5	5.47	?	?
SO_3	1.23	?	?
Cl	0.09	?	?
CO_2	5.14	?	?

Table 6: Blend3 particle properties from pelletized crushed feedstock. The crushed feedstock is used in the entrained flow reactor.

Property	Value	Description	Source
ρ	1,050 kg/m^3	particle density, daf basis	[7]
η	0.27	particle porosity	
k	0.23 W/mK	thermal conductivity	

Table 7: Entrained flow reactor yields for Blend3 feedstock.

Yield	wt. %
total liquid	64.9
char	13.9 ± 0.1
gas	17.2 ± 0.2
mass balance	96.9 ± 1.5
carbon balance	93.0 ± 1.0

2.3 Forest residue feedstock

The forest residue feedstock is comprised of branches/twigs, cambium, needles, bark, and whitewood. This feedstock is used in the NREL fluidized bed reactor (FBR) for the purposes of the FCIC project. The FBR is operated at fast pyrolysis conditions for the thermochemical conversion of biomass. The reactor is sometimes referred to as the 2FBR.

Table 8: General information for the forest residue feedstock.

Item	Description
Name	forest residue
ID	?
Contact	?

Table 9: Bark ultimate analysis mass percent, dry ash-free basis. Source [1].

Element	% daf	% daf	% daf
C	48.27	?	?
H	5.72	?	?
N	0.52	?	?

Table 10: Branches/twigs ultimate analysis mass percent, dry ash-free basis. Source [1].

Element	% daf	% daf	% daf
C	49.69	?	?
H	6.36	?	?
N	0.25	?	?

Table 11: Cambium ultimate analysis mass percent, dry ash-free basis. Source [1].

Element	% daf	% daf	% daf
C	48.52	?	?
H	6.39	?	?
N	0.11	?	?

Table 12: Needles ultimate analysis mass percent, dry ash-free basis. Source [1].

Element	% daf	% daf	% daf
C	48.59	?	?
H	5.92	?	?
N	1.22	?	?

Table 13: Whitewood ultimate analysis mass percent, dry ash-free basis. Source [1].

Element	% daf	% daf	% daf
C	48.27	?	?
H	6.15	?	?
N	0.10	?	?

Table 14: Whitewood biomass composition mass percent, dry basis. Source [2].

Component	% dry
Cellulose	38.04
Hemicellulose	24.2

3   Model development

Details about the biomass pyrolysis kinetics, biomass characterization method, and computational models developed for the entrained flow reactor are discussed in the following sections.

3.1   Pyrolysis kinetics

The kinetic reaction mechanisms presented in the Debiagi et al. 2018 paper are used to model biomass pyrolysis in the entrained flow reactor [4]. Table 15

summarizes the reactions along with the associated prefactors and activation energies. A description of the chemical species in the Debiagi et al. kinetic scheme is provided in Table 16. Species are grouped into solid, metaplastic, gas, and liquid phases.

Table 15: Kinetic reactions for biomass pyrolysis where A is the prefactor, E is the activation energy, and T is temperature. Source [4].

Item	Reaction	A (1/s)	E (cal/mol)
1	CELL → CELLA	1.5×10^{14}	47,000
2	CELLA → 0.40 CH2OHCHO + 0.03 CHOCHO + 0.17 CH3CHO + 0.25 C6H6O3 + 0.35 C2H5CHO + 0.20 CH3OH + 0.15 CH2O + 0.49 CO + 0.05 G{CO} + 0.43 CO2 + 0.13 H2 + 0.93 H2O + 0.05 G{COH2} loose + 0.02 HCOOH + 0.05 CH2OHCH2CHO + 0.05 CH4 + 0.1 G{H2} + 0.66 CHAR	2.5×10^{6}	19,100
3	CELLA → C6H10O5	$3.3 \times T$	10,000
4	CELL → 4.45 H2O + 5.45 CHAR + 0.12 G{COH2} stiff + 0.18 G{COH2} loose + 0.25 G{CO} + 0.125 G{H2} + 0.125 H2	9.0×10^{7}	31,000
5	GMSW → 0.70 HCE1 + 0.30 HCE2	1.0×10^{10}	31,000
6	XYHW → 0.35 HCE1 + 0.65 HCE2	1.25×10^{11}	31,400
7	XYGR → 0.12 HCE1 + 0.88 HCE2	1.25×10^{11}	30,000
8	HCE1 → 0.25 C5H8O4 + 0.25 C6H10O5 + 0.16 FURFURAL + 0.13 C6H6O3 + 0.09 CO2 + 0.1 CH4 + 0.54 H2O + 0.06 CH2OHCH2CHO + 0.1 CHOCHO + 0.02 H2 + 0.1 CHAR	$16.0 \times T$	12,900
9	HCE1 → 0.4 H2O + 0.39 CO2 + 0.05 HCOOH + 0.49 CO + 0.01 G{CO} + 0.51 G{CO2} + 0.05 G{H2} + 0.4 CH2O + 0.43 G{COH2} loose + 0.3 CH4 + 0.325 G{CH4} + 0.1 C2H4 + 0.075 G{C2H4} + 0.975 CHAR + 0.37 G{COH2} stiff + 0.1 H2 + 0.2 G{C2H6}	$3.0 \times 10^{-3} \times T$	3,600
10	HCE2 → 0.3 CO + 0.5125 CO2 + 0.1895 CH4 + 0.5505 H2 + 0.056 H2O + 0.049 C2H5OH + 0.035 CH2OHCHO + 0.105 CH3CO2H + 0.0175 HCOOH + 0.145 FURFURAL + 0.05 G{CH4} + 0.105 G{CH3OH} + 0.1 G{C2H4} + 0.45 G{CO2} + 0.18 G{COH2} loose + 0.7125 CHAR + 0.21 G{H2} + 0.78 G{COH2} stiff + 0.2 G{C2H6}	7.0×10^{9}	30,500
11	LIGH → LIGOH + 0.5 C2H5CHO + 0.4 C2H4 + 0.2 CH2OHCHO + 0.1 CO + 0.1 C2H6	6.7×10^{12}	37,500
12	LIGO → LIGOH + CO2	3.3×10^{8}	25,500
13	LIGC → 0.35 LIGCC + 0.1 VANILLIN + 0.1 C6H5OCH3 + 0.27 C2H4 + H2O + 0.17 G{COH2} loose + 0.4 G{COH2} stiff + 0.22 CH2O + 0.21 CO + 0.1 CO2 + 0.36 G{CH4} + 5.85 CHAR + 0.2 G{C2H6} + 0.1 G{H2}	1.0×10^{11}	37,200
14	LIGCC → 0.25 VANILLIN + 0.15 CRESOL + 0.15 C6H5OCH3 + 0.35 CH2OHCHO + 0.7 H2O + 0.45 CH4 + 0.3 C2H4 + 0.7 H2 + 1.15 CO + 0.4 G{CO} + 6.80 CHAR + 0.4 C2H6	1.0×10^{4}	24,800
15	LIGOH → 0.9 LIG + H2O + 0.1 CH4 + 0.6 CH3OH + 0.3 G{CH3OH} + 0.05 CO2 + 0.65 CO + 0.6 G{CO} + 0.05 HCOOH + 0.45 G{COH2} loose + 0.4 G{COH2} stiff + 0.25 G{CH4} + 0.1 G{C2H4} + 0.15 G{C2H6} + 4.25 CHAR + 0.025 C24H28O4 + 0.1 C2H3CHO	1.5×10^{8}	30,000
16	LIG → VANILLIN + 0.1 C6H5OCH3 + 0.5 C2H4 + 0.6 CO + 0.3 CH3CHO + 0.1 CHAR	$4.0 \times T$	12,000
17	LIG → 0.6 H2O + 0.3 CO + 0.1 CO2 + 0.2 CH4 + 0.4 CH2O + 0.2 G{CO} + 0.4 G{CH4} + 0.5 G{C2H4} + 0.4 G{CH3OH} + 1.25 G{COH2} loose + 0.65 G{COH2} stiff + 6.1 CHAR + 0.1 G{H2}	$8.3 \times 10^{-2} \times T$	8,000
18	LIG → 0.6 H2O + 2.6 CO + 0.6 CH4 + 0.4 CH2O + 0.75 C2H4 + 0.4 CH3OH + 4.5 CHAR + 0.5 C2H6	1.5×10^{9}	31,500
19	TGL → C2H3CHO + 2.5 MLINO + 0.5 U2ME12	7.0×10^{12}	45,700
20	TANN → 0.85 C6H5OH + 0.15 G{C6H5OH} + G{CO} + H2O + ITANN	2.0×10^{1}	10,000

21	ITANN $\rightarrow$ 5 CHAR + 2 CO + H2O + 0.55 G{COH2} loose + 0.45 G{COH2} stiff	1.0×10^3	25,000
22	G{CO2} $\rightarrow$ CO2	1.0×10^6	24,500
23	G{CO} $\rightarrow$ CO	5.0×10^{12}	52,500
24	G{CH3OH} $\rightarrow$ CH3OH	2.0×10^{12}	50,000
25	G{COH2}loose $\rightarrow$ 0.2 CO + 0.2 H2 + 0.8 H2O + 0.8 CHAR	6.0×10^{10}	50,000
26	G{C2H6} $\rightarrow$ C2H6	1.0×10^{11}	52,000
27	G{CH4} $\rightarrow$ CH4	1.0×10^{11}	53,000
28	G{C2H4} $\rightarrow$ C2H4	1.0×10^{11}	54,000
29	G{C6H5OH} $\rightarrow$ C6H5OH	1.5×10^{12}	55,000
30	G{COH2}stiff $\rightarrow$ 0.8 CO + 0.8 H2 + 0.2 H2O + 0.2 CHAR	1.0×10^9	59,000
31	G{H2} $\rightarrow$ H2	1.0×10^8	70,000
32	ACQUA $\rightarrow$ H2O	$1.0 \times T$	8,000

Table 16: Description of the chemical species in the Debiagi kinetics scheme for biomass pyrolysis. Source [4].

Item	Name	Formula	Phase	Description
1	CELL	$C_6H_{10}O_5$	solid	cellulose
2	CELLA	$C_6H_{10}O_5$	solid	active cellulose
3	GMSW	$C_5H_8O_4$	solid	hemicellulose softwood
4	XYHW	$C_5H_8O_4$	solid	hemicellulose hardwood
5	XYGR	$C_5H_8O_4$	solid	hemicellulose grass
6	HCE1	$C_5H_8O_4$	solid	intermediate hemicellulose
7	HCE2	$C_5H_8O_4$	solid	intermediate hemicellulose
8	ITANN	$C_8H_4O_4$	solid	intermediate phenolics
9	LIG	$C_{11}H_{12}O_4$	solid	intermediate lignin
10	LIGC	$C_{15}H_{14}O_4$	solid	carbon rich lignin
11	LIGCC	$C_{15}H_{14}O_4$	solid	intermediate lignin
12	LIGH	$C_{22}H_{28}O_9$	solid	hydrogen rich lignin
13	LIGO	$C_{20}H_{22}O_{10}$	solid	oxygen rich lignin
14	LIGOH	$C_{19}H_{22}O_8$	solid	intermediate lignin
15	TANN	$C_{15}H_{12}O_7$	solid	tannins
16	TGL	$C_{57}H_{100}O_7$	solid	triglycerides
17	CHAR	C	solid	char as pure carbon
18	G{COH2} loose	CH_2O	metaplastic	loose formaldehyde
19	G{CO2}	CO_2	metaplastic	trapped carbon dioxide
20	G{CO}	CO	metaplastic	trapped carbon monoxide
21	G{CH3OH}	CH_4O	metaplastic	trapped methanol
22	G{CH4}	CH_4	metaplastic	trapped methane
23	G{C2H4}	C_2H_4	metaplastic	trapped ethylene
24	G{C6H5OH}	C_6H_6O	metaplastic	trapped phenol
25	G{COH2} stiff	CH_2O	metaplastic	stiff formaldehyde
26	G{H2}	H_2	metaplastic	trapped hydrogen
27	G{C2H6}	C_2H_6	metaplastic	trapped ethane
28	C2H4	C_2H_4	gas	ethylene
29	C2H6	C_2H_6	gas	ethane
30	CH2O	CH_2O	gas	formaldehyde
31	CH4	CH_4	gas	methane
32	CO	CO	gas	carbon monoxide
33	CO2	CO_2	gas	carbon dioxide
34	H2	H_2	gas	hydrogen
35	C2H3CHO	C_3H_4O	liquid	acrolein

36	C2H5CHO	C_3H_6O	liquid	propionaldehyde
37	C2H5OH	C_2H_6O	liquid	ethanol
38	C5H8O4	$C_5H_8O_4$	liquid	xylofuranose
39	C6H10O5	$C_6H_{10}O_5$	liquid	levoglucosan
40	C6H5OCH3	C_7H_8O	liquid	anisole
41	C6H5OH	C_6H_6O	liquid	phenol
42	C6H6O3	$C_6H_6O_3$	liquid	hydroxymethylfurfural
43	C24H28O4	$C_{24}H_{28}O_4$	liquid	heavy molecular weight lignin
44	CH2OHCH2CHO	$C_3H_6O_2$	liquid	propionic acid
45	CH2OHCHO	$C_2H_4O_2$	liquid	acetic acid
46	CH3CHO	C_2H_4O	liquid	acetaldehyde
47	CH3CO2H	$C_2H_4O_2$	liquid	acetic acid
48	CH3OH	CH_4O	liquid	methanol
49	CHOCHO	$C_2H_2O_2$	liquid	glyoxal
50	CRESOL	C_7H_8O	liquid	cresol
51	FURFURAL	$C_5H_4O_2$	liquid	2-furaldehyde
52	H2O	H_2O	liquid	water from reactions
53	HCOOH	CH_2O_2	liquid	formic acid
54	MLINO	$C_{19}H_{34}O_2$	liquid	methyl linoleate
55	U2ME12	$C_{13}H_{22}O_2$	liquid	linalyl propionate
56	VANILLIN	$C_8H_8O_3$	liquid	vanillin
57	ACQUA	H_2O	liquid	water within biomass

3.2   Biomass characterization

The Debiagi kinetics rely on an initial biomass composition defined as cellulolose, hemicellulose, lignin-c, lignin-h, lignin-o, tannins, and triglycerides. According to the Debiagi et al. 2015 paper, the chemical components of the biomass are defined as shown below in Table 17 [5]. The Debiagi article does not provide information on how to experimentally determine these components; therefore, the reader must decide on appropriate measurement techniques.

Table 17: Chemical components of biomass according to Debiagi et al. [5].

Biomass composition	Description
cellulose	glucan
hemicellulose	mixture of sugars such as hexoses and pentoses; mainly xylose, mannose, galactose, and arabinose
lignin	aromatic alcohols such as coniferyl, sinapyl, p-coumaryl alcohol
lignin-c	carbon-rich lignin
lignin-h	hydrogen-rich lignin
lignin-o	oxygen-rich lignin
tannins	hydrophilic extractives, phenolics, ethanol and water, represented by a gallocatechin polymer
triglycerides	hydrophobic extractives, hexane and ether, linoleic acid

Ideally, the composition of the biomass would be directly measured; otherwise, the characterization method discussed in the Debiagi paper estimates the composition based on elemental analysis data [5]. The characterization method utilizes carbon and hydrogen obtained from elemental (ultimate) analysis of the biomass to predict the biochemical composition in terms of cellulose, hemicellulose, and lignin. Splitting parameters α, β, γ, δ, ϵ are used to improve the validity of the characterization procedure by accounting for extractives in the biomass.

3.3   Batch reactor

The material balance for a typical chemical reactor is shown in Equation 1 where C_0 is inlet concentration, C is outlet concentration, v is volumetric flow rate, r is the reaction rate, and V is the reactor volume.

$$accumulation = input - output + reaction$$
$$\frac{dC}{dt}V = vC_0 - vC + rV \qquad (1)$$

A batch reactor was modeled to understand the time scales associated with the biomass pyrolysis kinetics. For the batch reactor, input and output is zero therefore only the accumulation and reaction terms remain in the material balance. For a constant volumne reactor the V terms cancel out; therefore, Equation 2 represents the material balance for a batch reactor model.

$$accumulation = 0 - 0 + reaction$$

$$\frac{dC}{dt} = r \tag{2}$$

3.4 Sensitivity analysis

A sensitivity analysis was performed with the Debiagi pyrolysis kinetics to investigate the effects of biomass composition on product yields. The awesome SALib Python package was utilized for sample generation and prediction of the Sobol indices [6]. For the sensitivity analysis model, a sample represents the biomass composition as cellulose, hemicellulose, lignin-c, lignin-h, lignin-o, tannins, and triglycerides. This sample (or composition) is used in a reactor model at a certain temperature and pressure to predict pyrolysis yields. The sensitivity analysis model applies this approach to a large sample matrix then uses the generated data to perform a Sobol analysis.

4 Results and discussion

Characterization of the biomass along with batch reactor and sensitivity analysis results are discussed in this section.

4.1 Pyrolysis kinetics sensitivity analysis

A sensitivity analysis of the Debiagi pyrolysis kinetics in a batch reactor model was performed using 16,000 samples, a reaction time of 10 seconds, a reactor temperature of 773.15 K, and a reactor pressure of 101,325 Pa. Each sample represents some combination of cellulose, hemicellulose, lignin-c, lignin-h, lignin-o, tannins, and triglycerides. Batch reactor yields from the samples are shown in Figures 5 and 6. The Sobol sensitivity analysis based on the batch reactor results is presented in Figure 7.
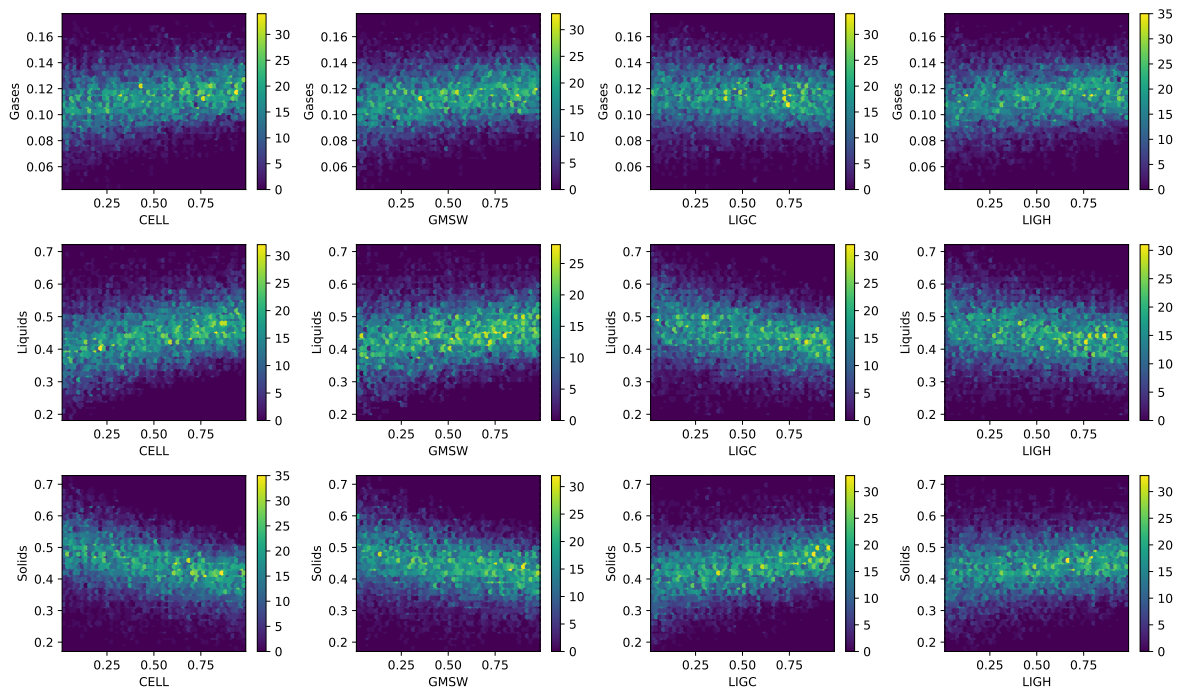
Figure 5: Batch reactor results for cellulose, hemicellulose (GMSW), carbon-rich lignin (LIGC), and hydrogen-rich lignin (LIGH) using 16,000 samples. Reaction time is 10 seconds at 773.15 K and 101,325 Pa. Colorbar represents bin count.
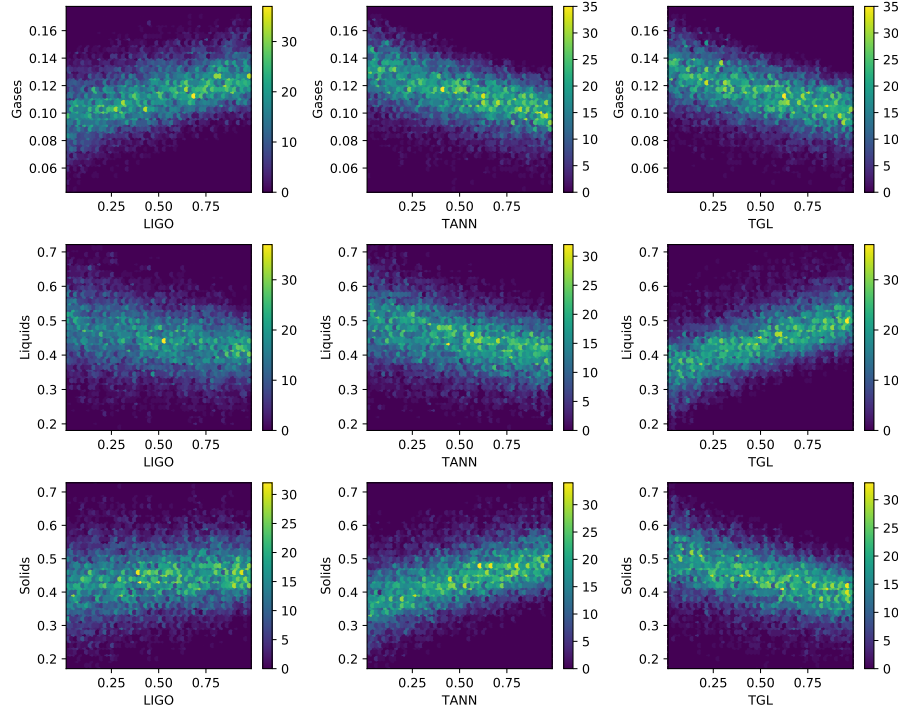
Figure 6: Batch reactor results for oxygen-rich lignin (LIGO), tannins (TANN), and triglycerides (TGL) using 16,000 samples. Reaction time is 10 seconds at 773.15 K and 101,325 Pa. Colorbar represents bin count.
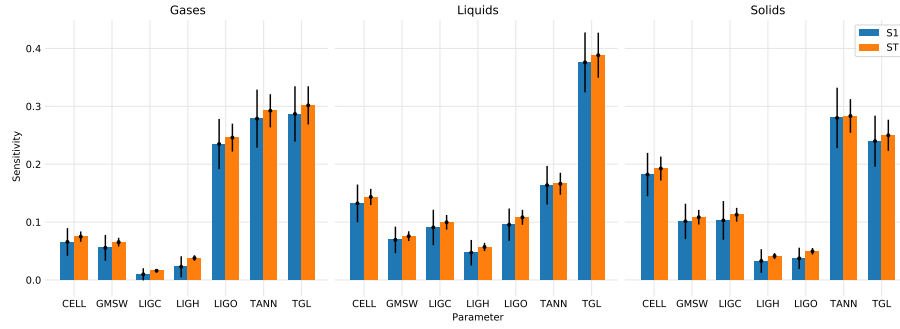

Figure 7: First-order (S1) and total-order (ST) Sobol indices for biomass composition with reactants grouped as gases, liquids, and solids using 16,000 samples.

4.2   Blend3 biomass composition

Several approaches were investigated to characterize the Blend3 feedstock for use with the Debiagi pyrolysis kinetics. The first approach uses the characterization method discussed in the Debiagi et al. 2015 paper where carbon and hydrogen from ultimate analysis is used to determine the biomass composition [5]. To use this approach for the Blend3 feedstock, the mass fraction of C and H on a dry ash-free basis (last column in Table 18) is used for the biomass characterization procedure.

Table 18: Ultimate analysis bases for the Blend3 feedstock. Mass percent values are given for as-received (ar), dry, and dry ash-free (daf) basis.

Element	% ar	% dry	% daf	% daf
C	49.52	52.70	53.06	53.16
H	5.28	5.62	5.66	5.67
O	38.35	40.82	41.10	41.17
N	0.15	0.16	0.16	
S	0.02	0.02	0.02	
ash	0.64	0.68		
moisture	6.04			

Case 1: The first approach to characterize the Blend3 feedstock was performed using a carbon mass fraction of 53.16%, hydrogen mass fraction of 5.67%, and splitting parameters $\alpha = 0.6$, $\beta = 0.8$, $\gamma = 0.8$, $\delta = 1.0$, and $\epsilon = 1.0$ which do not account for extractives in the feedstock. Results from this characterization are shown in Figure 8 and the associated biomass composition is given in Table 19. While this approach is useful for limited feedstock data, its accuracy is questionable when compared to experimental measurements. For example, chemical analysis of the Blend3 feedstock provides a lignin composition of 29.48% (see Table 4) whereas the characterization method using ultimate analysis data estimates a total lignin composition greater than 59%.
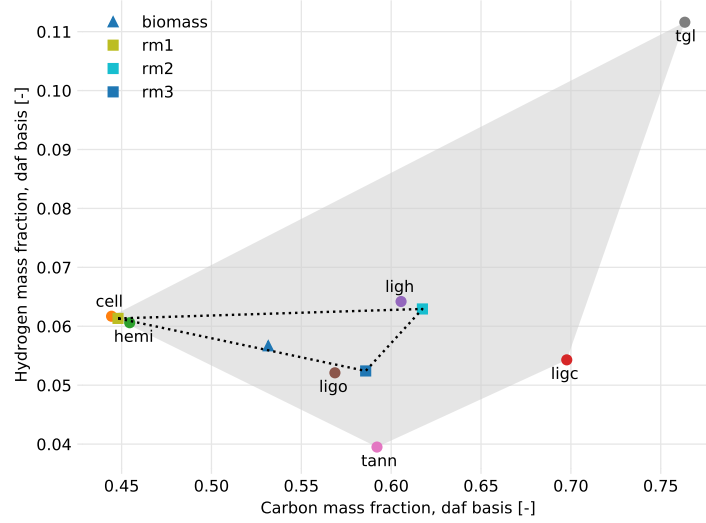
Figure 8: Characterization of the Blend3 feedstock using ultimate analysis data. Reference mixtures (rm) are labeled with square markers.

Case 2: To improve the Blend3 characterization based on ultimate analysis data, the splitting parameters were adjusted to account for extractives in the feedstock by using $\alpha = 0.56$, $\beta = 0.6$, $\gamma = 0.6$, $\delta = 0.78$, and $\epsilon = 0.88$. Also, since the uncertainty in the ultimate analysis data is unknown (see Table 3) the carbon mass fraction was adjusted to 51% and the hydrogen mass fraction to 6%. Results from these adjustments are presented in Figure 9 and Table 19.
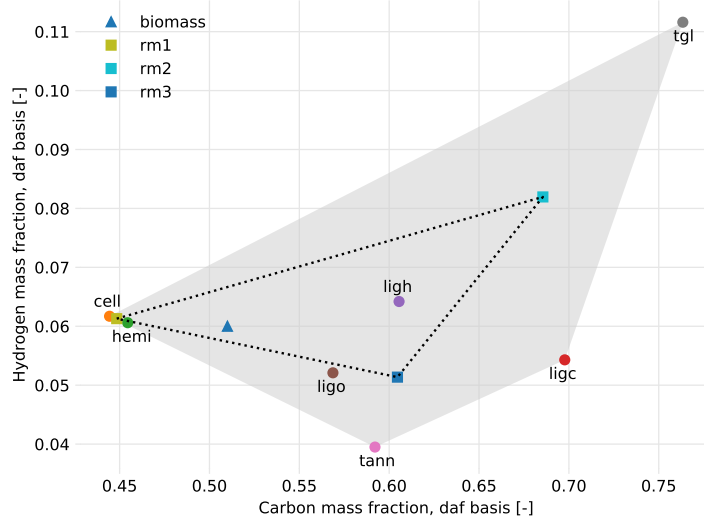
Figure 9: Characterization of the Blend3 feedstock using modified ultimate analysis data and adjusting the splitting parameters to account for extractives. Reference mixtures (rm) are labeled with square markers.

Case 3: The final approach to characterize the Blend3 feedstock, was to use chemical analysis data (see Table 4) to determine the biomass composition. Cellulose is represented by glucan while hemicellulose is comprised of arabinan, galactan, mannan, xylan, free fructose, free glucose, and sucrose. The measurement technique to determine the lignin components is unknown; therefore, the lignin is evenly divided into the carbon, hydrogen, and oxygen fractions. Tannins are represented by acetyl, water extractives, and ethanol extractives while ash is the non-structural and structural inorganics. Finally, the biomass composition based on the chemical analysis measurements is given in Table 19.

Table 19: Biomass composition for the Blend3 feedstock. Values are reported as mass percent on a dry ash-free basis (% daf).

Biomass composition	Case 1	Case 2	Case 3
cellulose	26.38	39.24	39.19
hemicellulose	14.33	25.12	23.26
lignin-c	7.84	8.57	9.89
lignin-h	5.27	3.11	9.89
lignin-o	46.18	18.00	9.89
tannins	0.00	2.95	7.88
triglycerides	0.00	3.01	0.00

4.3 Blend3 batch reactor conversion and yields

Here.

5 Conclusions

Here.

6 Source code

The Python code used to develop the models and generate results discussed in this paper is available on GitHub at `https://github.com/ccpcode/nrel-efr`.

7 Computational resources

An Apple MacBook Pro laptop was used to develop all the models and generate all the results discussed in this paper. A summary of the hardware is listed below:

- Model: MacBook Pro (16-inch, 2019)

- Processor: 2.6 GHz 6-Core Intel i7

- Memory: 32 GB 2667 MHz DDR4

- Integrated Graphics: Intel UHD Graphics 630

- Discrete Graphics: 4GB AMD Radeon Pro 5500M

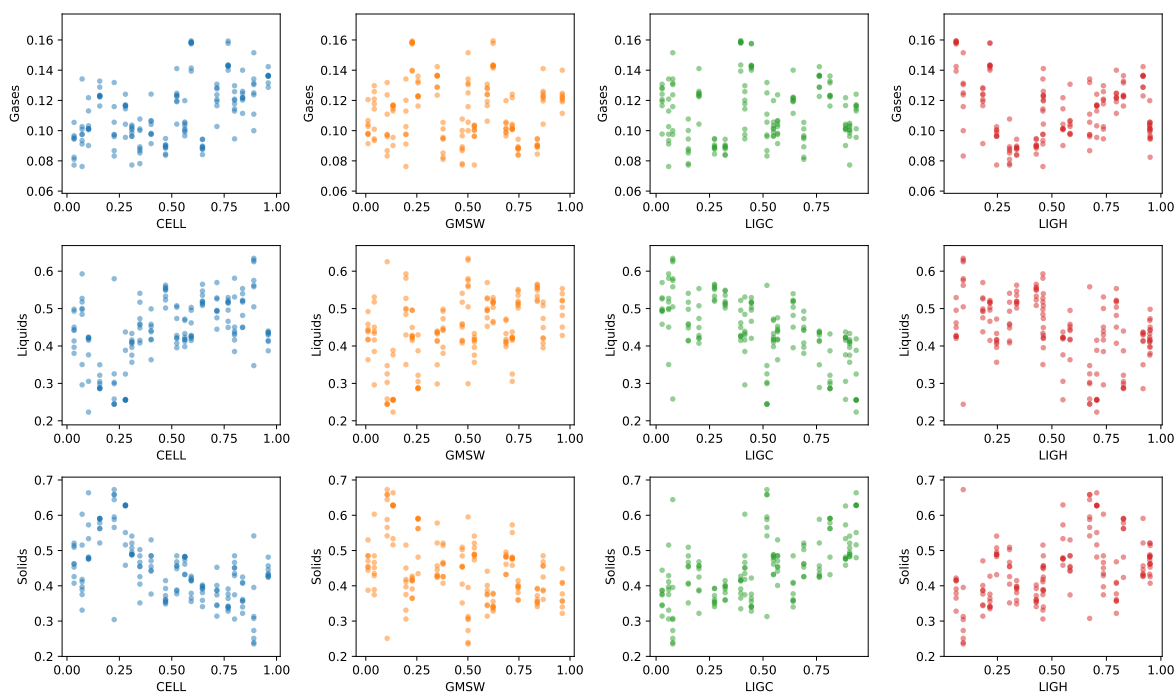# A Appendix

A.1 Sensitivity analysis

Figure 10: Batch reactor results for cellulose, hemicellulose (GMSW), carbon-rich lignin (LIGC), and hydrogen-rich lignin (LIGH) using 160 samples. Reaction time is 10 seconds at 773.15 K and 101,325 Pa.
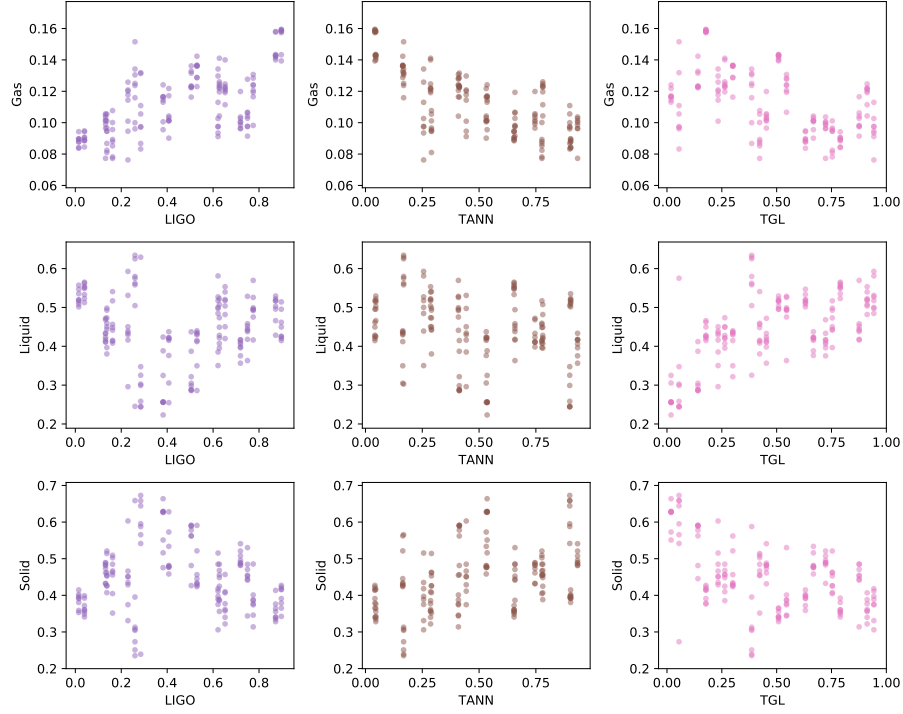
Figure 11: Batch reactor results for oxygen-rich lignin (LIGO), tannins (TANN), and triglycerides (TGL) using 160 samples. Reaction time is 10 seconds at 773.15 K and 101,325 Pa.
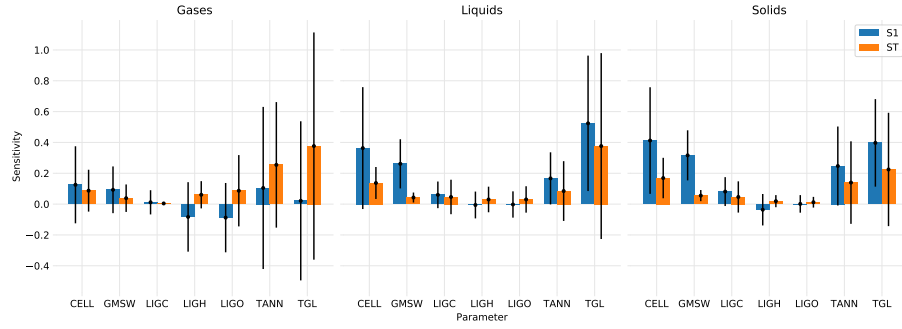

Figure 12: First-order (S1) and total-order (ST) Sobol indices for biomass composition with reactants grouped as gases, liquids, and solids using 160 samples.

References

[1] Unknown Author. *CHN Analysis Report*. Tech. rep. From Excel spreadsheet `jw-pine-chn-report-jw190920`. Unknown institution, 2019.

[2] Unknown Author. *Summary normalized*. Tech. rep. From Excel spreadsheet `summary-normalized`. Unknown institution, 2020.

[3] Mike Choratch. *Proximate and ultimate analysis*. Tech. rep. From PDF `chns_ipc_ms_blend3_nrel2017`. Hazen Research, Inc, 2017.

[4] P. Debiagi et al. "A predictive model of biochar formation and characterization". In: *Journal of Analytical and Applied Pyrolysis* 134 (2018), pp. 326–335.

[5] Paulo Eduardo Amaral Debiagi et al. "Extractives Extend the Applicability of Multistep Kinetic Scheme of Biomass Pyrolysis". In: *Energy & Fuels* 29.10 (2015), pp. 6544–6555.

[6] Jon Herman and Will Usher. "SALib: An open-source Python library for Sensitivity Analysis". In: *Journal of Open Source Software* 2.9 (2017), p. 97. DOI: `10.21105/joss.00097`. URL: `https://doi.org/10.21105/joss.00097`.

[7] M. Brennan Pecha et al. "Integrated Particle- and Reactor-Scale Simulation of Pine Pyrolysis in a Fluidized Bed". In: *Energy & Fuels* 32.10 (2018), pp. 10683–10694.

[8] Anne Starace and Justin Sluiter. *Compositional analysis Blend3*. Tech. rep. From Excel spreadsheet `comp_analysis_blend3_fy17verification`. National Renewable Energy Laboratory, 2020.